ESAIM: PROCEEDINGS, October 2011, Vol. 32, p. 56-75
E. Cancès, N. Crouseilles, H. Guillard, B. Nkonga, and E. Sonnendrücker, Editors

AN ASYMPTOTIC PRESERVING SCHEME FOR P_1 MODEL USING CLASSICAL DIFFUSION SCHEMES ON UNSTRUCTURED POLYGONAL MESHES

Emmanuel Franck[1], Philippe Hoch[2], Pierre Navaro[3] and Gérald Samba[4]

Abstract. A new scheme for discretizing the P_1 model on unstructured polygonal meshes is proposed. This scheme is designed such that its limit in the diffusion regime is the MPFA-O scheme which is proved to be a consistent variant of the Breil-Maire diffusion scheme. Numerical tests compare this scheme with a derived GLACE scheme for the P_1 system.

Résumé. Un nouveau schéma de discrétisation du modèle P_1 sur maillage non structuré composé de polygones est proposé. Ce schéma est construit pour que sa limite en régime diffusion soit le schéma MPFA-O qu'on démontre être une variante consistante du schéma de diffusion de Breil-Maire. Ce schéma est comparé sur des cas tests avec un schéma dérivé du schéma GLACE pour le modèle P_1.

Introduction

For the fusion by inertial confinement (ICF), photons play a major role in the ablation process responsible for the combustion of the Deuterium Tritium pellet.

For simplicity, we make the grey hypothesis and neglect Thomson scattering. Then, the propagation of photons can be modelized by the following equation

$$\left\{\begin{array}{c} \frac{1}{c}\partial_t I_\varepsilon(t,\mathbf{x},\mathbf{\Omega}) + \frac{1}{\varepsilon}\mathbf{\Omega}.\nabla I_\varepsilon(t,\mathbf{x},\mathbf{\Omega}) = \frac{\sigma}{\varepsilon^2}(\frac{1}{4\pi}acT_\varepsilon^4 - I_\varepsilon) \\ \partial_t(\rho C_v T_\varepsilon) = \frac{\sigma}{\varepsilon^2}(\int I_\varepsilon(\mathbf{\Omega})d\Omega - acT_\varepsilon^4) \end{array}\right. \tag{1}$$

where $I_\varepsilon(t,\mathbf{x},\mathbf{\Omega}) \geq 0$ is the radiative intensity in $\mathbf{x}$ for a unit vector direction $\mathbf{\Omega}$, $\sigma(\mathbf{x})$ a material dependent constant, T_ε the matter temperature, ρ the density, C_v the heat capacity, c the speed of light, a the radiative constant, ε a scaling coefficient.

When ε tends to zero (the medium becomes opaque), it is well known [DL04] that I_ε tends to $\frac{acT^4}{4\pi}$ where T is solution of the Rosseland equation

$$\partial_t(\rho C_v T + aT^4) - \nabla.\frac{ac}{3\sigma}\nabla T^4 = 0 \tag{2}$$

The ablation process is highly Rayleigh-Taylor unstable and sources of hydrodynamic instabilities must be carefully taken into account. It is important that the numerical methods to discretize

[1] CEA, DAM, DIF, Bruyères-le-Chatel, F-91297 Arpajon Cedex
[2] CEA, DAM, DIF, Bruyères-le-Chatel, F-91297 Arpajon Cedex
[3] IRMA, Strasbourg University
[4] CEA, DAM, DIF, Bruyères-le-Chatel, F-91297 Arpajon Cedex

(1) do not generate asymmetries. Monte-Carlo methods because of their statistical noise may give numerical instabilities of high mode number whereas approximation models such S_n models because they do not preserve the rotational invariance of the original equation (1) may be responsible for instabilities of low mode number. Flux limited diffusion models preserve the rotational invariance but are not accurate enough in transparent media (ε not small). P_n models do not suffer from these defaults but do not ensure the positivity of the radiative energy. This defect may be corrected by using non linear closures [DF99] which give at the lowest order the M_1 model. Let us mention other closures which take into account the geometry of the problem and may be more accurate in ICF simulation [CM08].

The materials involved in ICF may be transparent or opaque for the photons. As it has been said, the solution of the transport equation or its approximation models tends to the solution of the diffusion equation (2) when ε tends to zero. It is crucial that the numerical scheme obtains this solution with a mesh size not depending on ε. Such schemes will be said to preserve the diffusion limit or to be Asymptotic Preserving (AP schemes). This type of schemes is very useful in physical situation like the radiative transfer [BDF10, GT02, BD06, BCT08, BC07] but also in hydrodynamics with friction [JL96, CGRS08, BOP07] or biological model [Gos10].

On cartesian grids, a discretization of the M_1 model preserving the diffusion limit in opaque media has been proposed [BCT08] but no scheme with such property has been designed for unstructured meshes. Hydrodynamics codes such GO++ may generate at each time step new polygonal meshes adapted to the distortions of the fluid [Hoc02, Hoc11]. Such cells come out from successive refinement, derefinement and reconnexion steps. This capability is well adapted to ICF simulation since thin shells suffering large displacements are involved. Moreover, a locally very fine mesh is required to well describe the hydrodynamic unstable interfaces. For this reason, we want to construct numerical methods valid on unstructured polygonal meshes. The schemes described in the following have been implemented in this code. In this article, we address a simpler but not yet addressed issue. How to construct an AP scheme to discretize the P_1 model on unstructured polygonal meshes. First let see how we obtain this model from (1).

Defining $E_\varepsilon = \dfrac{1}{c}\displaystyle\int I_\varepsilon(\mathbf{\Omega})d\Omega$, $\mathbf{F}_\varepsilon = \displaystyle\int \mathbf{\Omega} I_\varepsilon(\mathbf{\Omega})d\Omega$, taking the zeroth and the first moment of the transport equation (1) and suppose that I_ε can be developed on its zeroth and first moments, one obtains

$$\begin{cases} \partial_t E_\varepsilon + \dfrac{1}{\varepsilon}\nabla.\mathbf{F}_\varepsilon = \dfrac{\sigma}{\varepsilon^2}c(aT_\varepsilon^4 - E_\varepsilon) \\ \partial_t \mathbf{F}_\varepsilon + \dfrac{c^2}{3\varepsilon}\nabla.(E_\varepsilon I_d) = -\dfrac{c\sigma}{\varepsilon^2}\mathbf{F}_\varepsilon \\ \partial_t(\rho C_v T_\varepsilon) = \dfrac{\sigma}{\varepsilon^2}c(E_\varepsilon - aT_\varepsilon^4) \end{cases} \tag{3}$$

The coupling term between radiation and matter in (3) is very stiff because of the $\dfrac{\sigma}{\varepsilon^2}$ factor. Thus, treat it explicitly requires very small time steps. The Fleck method [FC71, DL04] first designed for the system (1) is a simple way to avoid this problem. It consists in predicting the temperature at the end of the time step by linearizing the matter internal energy equation around the temperature at the beginning of the time step $[t_n, t_{n+1}]$.

$\tilde{T}_\varepsilon^4 = \dfrac{1}{f_\varepsilon}((T^4)^n + \dfrac{f_\varepsilon - 1}{a}E_\varepsilon)$ with $f_\varepsilon = 1 + \dfrac{c\sigma 4a(T^3)^n\Delta t}{\varepsilon^2\rho C_v}$

Replacing T_ε^4 by $\tilde{T}_\varepsilon^4$ in the $\dfrac{\sigma}{\varepsilon^2}c(E_\varepsilon - aT_\varepsilon^4)$ terms in (3) leads to the system

$$\begin{cases} \partial_t E_\varepsilon + \dfrac{1}{\varepsilon}\nabla.\mathbf{F}_\varepsilon = \dfrac{\sigma}{f_\varepsilon\varepsilon^2}c(a(T^4)^n - E_\varepsilon) \\ \partial_t \mathbf{F}_\varepsilon + \dfrac{c^2}{3\varepsilon}\nabla.(E_\varepsilon I_d) = -\dfrac{c\sigma}{\varepsilon^2}\mathbf{F}_\varepsilon \\ \partial_t(\rho C_v T_\varepsilon) = \dfrac{\sigma}{f_\varepsilon\varepsilon^2}c(E_\varepsilon - a(T^4)^n) \end{cases} \tag{4}$$

The coupling term in (4) is not as stiff as in (3) since $f_\varepsilon\varepsilon^2 = o(1)$. When ε tends to zero, $(E_\varepsilon, T_\varepsilon)$ tends to (E, T) solution of the following system on the time step $[t_n, t_{n+1}]$

$$\left\{ \begin{array}{c} \partial_t(\rho C_v T + E) - \nabla.\frac{c}{3\sigma}\nabla E = 0 \\ \partial_t(E) - \nabla.\frac{c}{3\sigma}\nabla E = \frac{\sigma}{\hat{f}} c(a(T^4)^n - E) \end{array} \right. \tag{5}$$

with $\hat{f} = \frac{c\sigma 4a(T^3)^n \Delta t}{\rho C_v}$. E satisfies a diffusion equation but the equality $E = aT^4$ cannot be proved, thus (2) is not obtained. Nevertheless, this widely used method generates correct solutions in most situations [DL04]. But stiff terms are still present in (4) which implies using an AP scheme to ensure at the discrete level the convergence of (4) to (5).

We will take a simpler model which retains the main features of (4). We assume that σ is constant in the rest of the paper. We think this is not restrictive since handling with non constant σ is straightforward in the limit diffusion schemes. We rescale the P_1 equations without constant coefficients thus obtaining

$$\left\{ \begin{array}{c} \partial_t E_\varepsilon + \dfrac{1}{\varepsilon}\nabla.\mathbf{F}_\varepsilon = 0 \\ \partial_t \mathbf{F}_\varepsilon + \dfrac{1}{\varepsilon}\nabla.(E_\varepsilon I_d) = -\dfrac{\sigma}{\varepsilon^2}\mathbf{F}_\varepsilon \end{array} \right. \tag{6}$$

When ε tends to zero, this equation tends towards the following diffusion equation

$$\partial_t E(t,\mathbf{x}) - \frac{1}{\sigma}\triangle E(t,\mathbf{x}) = 0 \tag{7}$$

A first idea to solve (6) is to take schemes first designed for the Euler equations and to adapt them to solve the P_1 model.

In [BDF10] AP schemes based on the GLACE scheme [Maz07, CDDL09] on unstructured meshes for this model have been constructed. In section 1, these schemes are presented. But these schemes exhibit spurious modes on cartesian meshes. For this reason, we propose a different way to obtain AP scheme for the P_1 system.

The idea is to target well-known diffusion schemes used in the ICF context. We adapt them to solve the P_1 model in such a way that their diffusion limit is the aimed diffusion scheme.

We aim the Breil-Maire scheme [BM06] because of its interesting properties. In this scheme, the radiative energy is cell centered which is nice for coupling with schemes handling thermodynamical centered quantities to solve Euler equations. It converges at the second order on most types of meshes at the notable exception of the random meshes. On cartesian meshes, it gives the classical five-point scheme which does not have spurious modes. In this paper, a variant of this scheme is designed to make it consistent on all kinds of meshes. In section 2, we describe the Breil-Maire scheme and its variant. In section 3, we propose two AP schemes for the P_1 system, the first one has the Breil-Maire scheme as diffusion limit, the second one its consistent variant. In section 4, we compare these schemes on two cases.

1. GLACE asymptotic preserving schemes

In this section we redefine the GLACE asymptotic preserving schemes constructed in [BDF10] for the P_1 model.

1.1. Notations

We consider an unstructured mesh in dimension 2. The mesh is defined by a finite number of vertices $\mathbf{x}_r$ and polygonal cells Ω_j. We denote $\mathbf{x}_j$ the gravity center of Ω_j. The vertices are denoted $\mathbf{x}_{\ldots,r-1,r,r+1,\ldots}$. In each cell j, we define the length and the normal associated to the node of local index r (Fig .1). (x_r, y_r) are the coordinates of $\mathbf{x}_r$. We also define

$$l_{jr} = \frac{1}{2} \parallel \mathbf{x}_{r+1} - \mathbf{x}_{r-1} \parallel \text{ and } \mathbf{n}_{jr} = \frac{1}{2l_{jr}} \begin{pmatrix} -y_{r-1} + y_{r+1} \\ x_{r-1} - x_{r+1} \end{pmatrix}. \tag{8}$$

Remark 1. *The letters j denote always the index on a cell and the letter r is always the index on a node.*

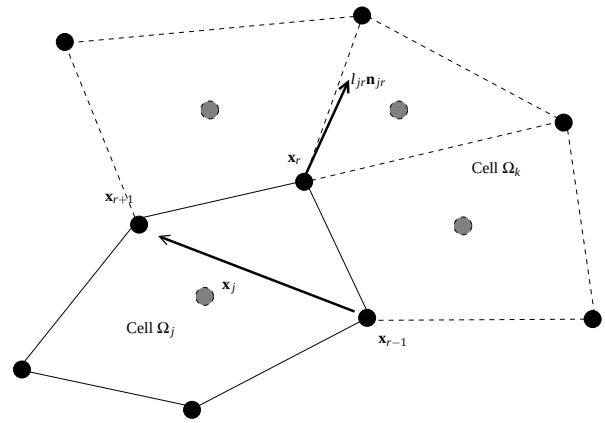

FIGURE 1. Notation for node formulation. The corner length l_{jr} and the corner normal $\mathbf{n}_{jr}$ are defined in equation (8).

1.2. Asymptotic preserving schemes

To construct an asymptotic preserving scheme on unstructured meshes, the idea is to use the nodal scheme "GLACE" constructed for linearized Euler equations, by analogy with the P_1 model and use the Jin-Levermore method [JL96] to make it AP. The Jin-Levermore procedure consists in incorporating the stationary states associated to fluxes. This method gives the following GLACE AP schemes.

Definition 2. *The scheme JL-(a)*

$$\left\{\begin{array}{c} \mid \Omega_j \mid \partial_t E_j(t) + \dfrac{1}{\varepsilon}\displaystyle\sum_r l_{jr}(\mathbf{F}_r, \mathbf{n}_{jr}) = 0 \\ \mid \Omega_j \mid \partial_t \mathbf{F}_j(t) + \dfrac{1}{\varepsilon}\displaystyle\sum_r \mathbf{G}_{jr} = - \mid \Omega_j \mid \dfrac{\sigma}{\varepsilon^2}\mathbf{F}_j \end{array}\right. \tag{9}$$

and the scheme JL-(b)

$$\left\{\begin{array}{c} \mid \Omega_j \mid \partial_t E_j(t) + \dfrac{1}{\varepsilon}\displaystyle\sum_r l_{jr}(\mathbf{F}_r, \mathbf{n}_{jr}) = 0 \\ \mid \Omega_j \mid \partial_t \mathbf{F}_j(t) + \dfrac{1}{\varepsilon}\displaystyle\sum_r \mathbf{G}_{jr} = -\dfrac{\sigma}{\varepsilon^2}\displaystyle\sum_r l_{jr}\mathbf{n}_{jr} \otimes (\mathbf{x}_r - \mathbf{x}_j)\mathbf{F}_r \end{array}\right. \tag{10}$$

with the fluxes

$$\left\{\begin{array}{c} \mathbf{G}_{jr} = l_{jr}E_j\mathbf{n}_{jr} + l_{jr}\widehat{\alpha}_{jr}(\mathbf{F}_j - \mathbf{F}_r) - \dfrac{\sigma}{\varepsilon}l_{jr}\mathbf{n}_{jr} \otimes (\mathbf{x}_r - \mathbf{x}_j)\mathbf{F}_r \\ \left(\displaystyle\sum_j l_{jr}\widehat{\alpha}_{jr} + \sum_j \dfrac{\sigma}{\varepsilon}(l_{jr}\mathbf{n}_{jr} \otimes (\mathbf{x}_r - \mathbf{x}_j))\right)\mathbf{F_r} = \displaystyle\sum_j (l_{jr}E_j\mathbf{n}_{jr} + l_{jr}\widehat{\alpha}_{jr}\mathbf{F_j}) \end{array}\right. \tag{11}$$

and $\widehat{\alpha}$ defined by

$$\widehat{\alpha}^I_{jr} = \mathbf{n}_{jr} \otimes \mathbf{n}_{jr}. \tag{12}$$

or

$$\widehat{\alpha}^{II}_{jr} = \frac{1}{2l_{jr}}(l_{jr-1,r}\mathbf{n}_{jr-1,r} \otimes \mathbf{n}_{jr-1,r} + l_{jr,r+1}\mathbf{n}_{jr,r+1} \otimes \mathbf{n}_{jr,r+1}) \tag{13}$$

with $l_{jr\pm}$, $\mathbf{n}_{jr\pm}$ are lengths and normals associated to the edges $[\mathbf{x}_{r-1}, \mathbf{x}_r]$ and $[\mathbf{x}_r, \mathbf{x}_{r+1}]$.

To obtain the JL-(a) scheme, we write the Riemann invariant

$$E_j + (\mathbf{F}_j, \mathbf{n}_{jr}) = E_{jr} + (\mathbf{F}_r, \mathbf{n}_{jr})$$

then E is extrapolated at the node r using
$\tilde{E}(\mathbf{x}_r) = E_j + ((\mathbf{x}_r - \mathbf{x}_j), \nabla E(\mathbf{x}_r))$ and the steady state relation $-\frac{\sigma}{\epsilon}\mathbf{F}(\mathbf{x}_r) = \nabla E(\mathbf{x}_r)$ (cf second equation of (6)).

Replacing E_j by $\tilde{E}(\mathbf{x}_r)$ in the Riemann invariant, one obtains

$$E_j + (\mathbf{F}_j, \mathbf{n}_{jr}) = E_{jr} + (\mathbf{F}_r, \mathbf{n}_{jr}) + \frac{\sigma}{\epsilon}((\mathbf{x}_r - \mathbf{x}_j), \mathbf{F}_r)$$

thus

$$E_{jr} = E_j + (\mathbf{F}_j - \mathbf{F}_r, \mathbf{n}_{jr}) - \frac{\sigma}{\epsilon}((\mathbf{x}_r - \mathbf{x}_j), \mathbf{F}_r)$$

we obtain the fluxes (11) using $\mathbf{G}_{jr} = l_{jr}E_{jr}\mathbf{n}_{jr}$ and $\sum_j \mathbf{G}_{jr} = 0$.

The JL-(b) consists in discretizing the source term using the fluxes. We write $\mathbf{F}_j$ as a mean of $\mathbf{F}_r$ since $|\Omega_j|I_d = \sum_r l_{jr}\mathbf{n}_{jr}\otimes(\mathbf{x}_r - \mathbf{x}_j)$. In 1D this manipulation in the Jin-Levermore scheme gives the Gosse-Toscani scheme. The JL-(b) scheme with $\widehat{\alpha}$ defined by the equation (12) can be seen as the 2D extension of the Gosse-Toscani scheme [GT02] originally defined only in 1D. The Gosse-Toscani scheme in 1D is the upwind scheme multiplied by a "magic" coefficient $M = \frac{2\varepsilon}{2\varepsilon+\sigma\Delta x}$. JL-(b) in 1D gives the upwind GLACE scheme multiplied by $M_2 = \frac{\sqrt{2}\varepsilon}{\sqrt{2}\varepsilon+\sigma\Delta x}$. The ratio $\sqrt{2}$ between M and M_2 corresponds to the ratio between the upwind GLACE viscosity and the classical upwind viscosity.

Remark 3. *The JL-(b) scheme is L^2 stable. For the JL-(a) scheme we cannot prove this property.*

In the following, we derive the JL-(b) scheme in another way. Starting from the system

$$\begin{cases} \mid \Omega_j \mid \partial_t E_j(t) + \frac{1}{\varepsilon}\sum_r l_{jr}(\mathbf{F}_r, \mathbf{n}_{jr}) = 0 \\ \mid \Omega_j \mid \partial_t \mathbf{F}_j(t) + \frac{1}{\varepsilon}\sum_r l_{jr}\mathbf{n}_{jr}E_{jr} = 0 \end{cases} \tag{14}$$

and

$$E_{jr} - E_j + ((\mathbf{F}_r - \mathbf{F}_j), \mathbf{n}_{jr}) = 0 \tag{15}$$

we look for a relation between E_{jr} and $\mathbf{F}_r$ allowing to discretize

$$\begin{cases} \nabla.\mathbf{F} = 0 \\ \nabla E + \frac{\sigma}{\varepsilon}\mathbf{F} = 0 \end{cases} \tag{16}$$

Using the Einstein convention on the repeated indices, the second equation of (16) may be rewritten

$$\frac{\partial}{\partial x_i}E + \frac{\sigma}{\varepsilon}F_l\frac{\partial}{\partial x_k}(x_l\delta_{ik}) = 0 \tag{17}$$

since $\frac{\partial}{\partial x_k}(x_l\delta_{ik}) = \delta_{il}$.

In this expression x_l designs the lth (l varies from 1 to 2 in 2D) coordinate of $\mathbf{x}$.

Now, we integrate the equation (17) on the control volume V_r (Fig .2). We replace x_l by the lth coordinate of $\mathbf{x_j}$ on each cell j. We set $\mathbf{F_r}$ constant on V_r which satisfies the first equation of (16) to obtain

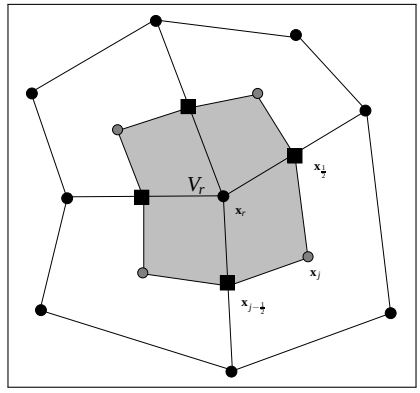

FIGURE 2. V_r is defined by the closed loop that joins the center of the cells $\mathbf{x_j}$ and the middle of the edges around the vertex $\mathbf{x_r}$

$$\sum_j l_{jr} E_{jr} \mathbf{n}_{jr} + \frac{\sigma}{\varepsilon} (\sum_j l_{jr} \mathbf{n}_{jr} \otimes \mathbf{x}_j) \mathbf{F_r} = 0 \tag{18}$$

Using (15) to eliminate E_{jr} in (18), one gets

$$\left(\sum_j l_{jr} \mathbf{n}_{jr} \otimes \mathbf{n}_{jr} - \frac{\sigma}{\varepsilon} \sum_j l_{jr} \mathbf{n}_{jr} \otimes \mathbf{x}_j \right) \mathbf{F_r} = \sum_j l_{jr} E_j \mathbf{n}_{jr} + \sum_j l_{jr} \mathbf{n}_{jr} \otimes \mathbf{n}_{jr} \mathbf{F_j} \tag{19}$$

This is exactly the expression of $\mathbf{F_r}$ in (11) since $\sum_j l_{jr} \mathbf{n}_{jr} = 0$.

Eliminating E_{jr} in (14), one obtains (10) with the same expression for $\mathbf{G}_{jr}$ with $\widehat{\alpha}$ defined by equation (12). We have thus obtained the JL-(b) scheme.

The existence of these schemes is verified if the matrix

$$\left(\sum_j l_{jr} \widehat{\alpha}_{jr} + \sum_j \frac{\sigma}{\varepsilon} (l_{jr} \mathbf{n}_{jr} \otimes (\mathbf{x}_r - \mathbf{x}_j)) \right)$$

is invertible. In [BDF10] we give sufficient condition verified by the mesh to have this property. For example for triangular meshes, if all the angles are superior to 10 degrees, the matrix is invertible. Numerically, we never have noted the non-invertibility of this matrix.

1.3. Limit diffusion scheme

To finish the definition of AP GLACE schemes we define the limit scheme. The previous schemes tend towards a new diffusion scheme.

Definition 4. *GLACE diffusion scheme*

$$\begin{cases} E_j'(t) + \dfrac{1}{\mid \Omega_j \mid} \displaystyle\sum_r l_{jr} \left(\mathbf{n}_{jr}, \mathbf{F}_r \right) = 0, \\ \sigma A_r \mathbf{F}_r = \displaystyle\sum_j l_{jr} \mathbf{n}_{jr} E_j, \qquad \textit{with } A_r = \displaystyle\sum_j l_{jr} \mathbf{n}_{jr} \otimes \left(\mathbf{x}_r - \mathbf{x}_j \right). \end{cases} \tag{20}$$

In [BDF10] we prove that if the solution is sufficiently smooth and the matrix A_r is positive the scheme converges at first order. However these schemes have a default. With a Dirac mass initial condition, they may exhibit spurious modes on cartesian mesh because of their cross stencil. For this reason we construct a new AP scheme with a limit scheme which has not this default.

2. Breil-Maire diffusion and MPFA-O scheme

In this section we define the Breil-Maire scheme [BM06] and we modify the local matrix used in this scheme to make it consistent. To finish we prove the equivalence between this scheme and the MPFA-O scheme.

Definition 5. *The Breil-Maire scheme defined by [BM06] is:*

$$\left\{\begin{array}{c} \mid \Omega_j \mid \partial_t E_j(t) + \sum_r \frac{1}{2}(l_{jr-1,r}\Phi^j_{r-1/2,r} + l_{jr,r+1}\Phi^j_{r,r+1/2}) = 0 \\ \frac{1}{2} l_k(\Phi^{k-1}_k + \Phi^k_k) = 0 \\ \begin{pmatrix} \Phi^j_{r-1/2,r} \\ \Phi^j_{r,r+1/2} \end{pmatrix} = -\frac{1}{\sigma}\frac{1}{2\omega^j_r} T^j_r \begin{pmatrix} l_{jr-1,r}(\bar{E}_{r-1/2,r} - E_j) \\ l_{jr,r+1}(\bar{E}_{r,r+1/2} - E_j) \end{pmatrix} \end{array}\right. \tag{21}$$

with

$$T^j_r = \begin{pmatrix} 1 & -\cos(\theta^j_r) \\ -\cos(\theta^j_r) & 1 \end{pmatrix} \tag{22}$$

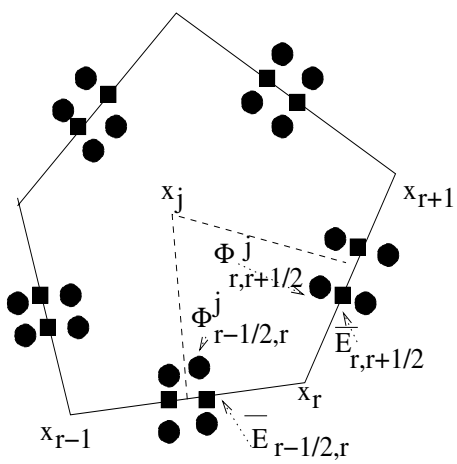

Figure 3. Breil-Maire scheme stencil

where ω^r_j is the area of the sub-cell associated to the r node and the j cell. We note $\mathbf{x}_{r+1/2}$ the middle of the segment $[\mathbf{x}_r, \mathbf{x}_{r+1}]$, and θ^j_r the angle between $\mathbf{x_r}$, $\mathbf{x}_{r+1/2}$ and $\mathbf{x}_{r-1/2}$.

The second equation ensures the continuity of the normal fluxes Φ^k_{k-1} and Φ^k_k at both sides of the k edge.

We assume that $\Phi^{k-1}_k = -\frac{1}{\sigma}(\nabla E, \mathbf{n}^k_{k-1})$. A variational formulation is used to obtain (22). It can be interpreted as assuming that the quadrilateral $\mathbf{x}_j\mathbf{x}_{r-1/2}\mathbf{x}_r\mathbf{x}_{r+1/2}$ is a parallelogram. The advantage of this formulation is that the tensor T^j_r is symmetric. This leads to a symmetric global matrix. The drawback is that the consistency is lost on some kinds of meshes as shown by the numerical results.

Now we want to modify the matrix T^j_r to obtain a consistent scheme.

2.1. The modified Breil-Maire and MPFA-O schemes

The last equation relates the two normal fluxes on the two edges in the sub-cell of j associated to the node r with the differences of the value E_j at the center of gravity O and the two midpoint edge values $\bar{E}_{r-1/2,r}$ and $\bar{E}_{r,r+1/2}$ (at A and C on the figure 4).

From

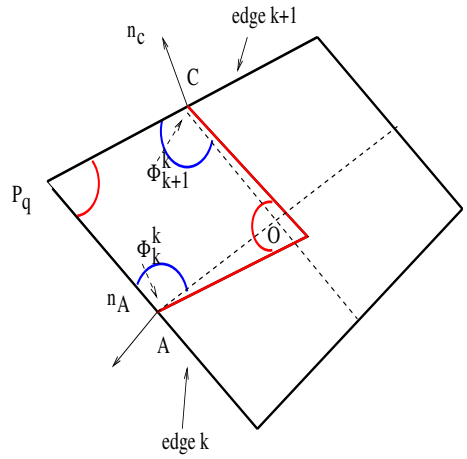

FIGURE 4. Breil-Maire scheme

$$\begin{cases} \mathbf{n}_A = \dfrac{(\mathbf{n}_A, \mathbf{OC}^\perp)}{(\mathbf{OA}, \mathbf{OC}^\perp)}\mathbf{OA} + \dfrac{(\mathbf{n}_A, \mathbf{OA}^\perp)}{(\mathbf{OC}, \mathbf{OA}^\perp)}\mathbf{OC} \\ \\ \mathbf{n}_C = \dfrac{(\mathbf{n}_C, \mathbf{OC}^\perp)}{(\mathbf{OA}, \mathbf{OC}^\perp)}\mathbf{OA} + \dfrac{(\mathbf{n}_C, \mathbf{OA}^\perp)}{(\mathbf{OC}, \mathbf{OA}^\perp)}\mathbf{OC} \end{cases}$$

one obtains

$$\begin{cases} \Phi_k^k = -\dfrac{1}{\sigma}(\nabla E, \mathbf{n}_A) \simeq \dfrac{1}{\sigma}\dfrac{1}{\beta}\Big((\mathbf{n}_A, \mathbf{OC}^\perp)(E(O) - E(A)) + (\mathbf{n}_A, \mathbf{OA}^\perp)(E(O) - E(C))\Big) \\ \\ \Phi_{k+1}^k = -\dfrac{1}{\sigma}(\nabla E, \mathbf{n}_C) \simeq \dfrac{1}{\sigma}\dfrac{1}{\beta}\Big((\mathbf{n}_C, \mathbf{OC}^\perp)(E(O) - E(A)) + (\mathbf{n}_C, \mathbf{OA}^\perp)(E(O) - E(C))\Big) \end{cases}$$

with $\mathbf{OA}^\perp = \begin{pmatrix} y_A - y_O \\ -(x_A - x_O) \end{pmatrix}$, $\mathbf{OC}^\perp = \begin{pmatrix} -(y_C - y_O) \\ x_C - x_O \end{pmatrix}$ et $\beta = (\mathbf{OA}, \mathbf{OC}^\perp) = (\mathbf{OC}, \mathbf{OA}^\perp)$. Therefore we obtain the new scheme

Definition 6. *The Breil-Maire modified scheme is*

$$\begin{cases} \mid \Omega_j \mid \partial_t E_j(t) + \displaystyle\sum_r \frac{1}{2}(l_{jr-1,r}\Phi^j_{r-1/2,r} + l_{jr,r+1}\Phi^j_{r,r+1/2}) = 0 \\ \frac{1}{2} l_k(\Phi_k^{k-1} + \Phi_k^k) = 0 \\ \begin{pmatrix} \Phi^j_{r-1/2,r} \\ \Phi^j_{r,r+1/2} \end{pmatrix} = -\dfrac{1}{\sigma}\dfrac{1}{2\omega_r^j} T_r^j \begin{pmatrix} l_{jr-1,r}(\bar{E}_{r-1/2,r} - E_j) \\ l_{jr,r+1}(\bar{E}_{r,r+1/2} - E_j) \end{pmatrix} \end{cases} \tag{23}$$

with

$$T_r^j = \begin{pmatrix} 2w_r^j \dfrac{(\mathbf{n}_{jr-1,r}, (\mathbf{x}_{r+1/2} - \mathbf{x}_j)^\perp)}{\beta l_{jr-1,r}} & 2w_r^j \dfrac{(\mathbf{n}_{jr-1,r}, (\mathbf{x}_{r-1/2} - \mathbf{x}_j)^\perp)}{\beta l_{jr,r+1}} \\ 2w_r^j \dfrac{(\mathbf{n}_{jr,r+1}, (\mathbf{x}_{r+1/2} - \mathbf{x}_j)^\perp)}{\beta l_{jr-1,r}} & 2w_r^j \dfrac{(\mathbf{n}_{jr,r+1}, (\mathbf{x}_{r-1/2} - \mathbf{x}_j)^\perp)}{\beta l_{jr,r+1}} \end{pmatrix} \tag{24}$$

and $\beta = ((\mathbf{x}_{r-1/2} - \mathbf{x}_j), (\mathbf{x}_{r+1/2} - \mathbf{x}_j)^\perp) = ((\mathbf{x}_{r-1/2} - \mathbf{x}_j)^\perp, (\mathbf{x}_{r+1/2} - \mathbf{x}_j))$

The difference with the original scheme lies in the definition of T_r^j. Now, the quadrilateral $\mathbf{x}_j\mathbf{x}_{r-1/2}\mathbf{x}_r\mathbf{x}_{r+1/2}$ is not assumed to be a parallelogram. The numerical results show that the consistency is recovered at the expense of the symmetry of the tensor T_r^j.

In both schemes, the edges unknowns can be eliminated. The resulting centered schemes have a nine points stencil on structured mesh composed of quadrilaterals and give the classical five-point scheme on cartesian meshes.

Proposition 7. *The modified Breil-maire scheme is the MPFA-O scheme defined by [ABBM98, AE06]*

Proof. We use the same notation. The MPFA-O scheme uses the previous type of discretization. The gradient is defined in the sub-cell of j associated to the node r.

$$\nabla E_j = \frac{\bar{E}_{r,r+1/2} - E_j}{2V_r^j}(\mathbf{x}_{r-1/2} - \mathbf{x}_j)^\perp + \frac{\bar{E}_{r-1/2,r} - E_j}{2V_r^j}(\mathbf{x}_{r+1/2} - \mathbf{x}_j)^\perp \tag{25}$$

with V_j^r the area of the triangle based on $\mathbf{x}_{r-1/2}$, $\mathbf{x}_{r+1/2}$ and $\mathbf{x}_j$.

To obtain the equivalence, we develop the third equation of (23), the area w_r^j and the length vanish. We remark that $\beta = 2V_r^j$ then we have

$$\begin{pmatrix} \Phi^j_{r-1/2,r} \\ \Phi^j_{r,r+1/2} \end{pmatrix} = \tag{26}$$

$$-\frac{1}{\sigma}\begin{pmatrix} \dfrac{(\mathbf{n}_{jr-1,r}, (\mathbf{x}_{r+1/2} - \mathbf{x}_j)^\perp)}{2V_r^j}(\bar{E}_{r-1/2,r} - E_j) + \dfrac{(\mathbf{n}_{jr-1,r}, (\mathbf{x}_{r-1/2} - \mathbf{x}_j)^\perp)}{2V_r^j}(\bar{E}_{r,r+1/2} - E_j) \\ \dfrac{(\mathbf{n}_{jr,r+1}, (\mathbf{x}_{r+1/2} - \mathbf{x}_j)^\perp)}{2V_r^j}(\bar{E}_{r-1/2,r} - E_j) + \dfrac{(\mathbf{n}_{jr,r+1}, (\mathbf{x}_{r-1/2} - \mathbf{x}_j)^\perp)}{2V_r^j}(\bar{E}_{r,r+1/2} - E_j) \end{pmatrix} \tag{27}$$

ϕ discretizes the gradient using the same formula as MPFA-O but in the normal direction. Therefore the continuity conditions of the two schemes are equivalent. □

The Breil-Maire scheme is symmetric, the local matrices are always invertible, but it is not consistent. The MPFA-O scheme is consistent but the local matrices associated to the continuity condition are not always invertible theoretically and numerically (we can find an example in [MV06]). Now we want to construct an AP scheme with these schemes as diffusion limit.

3. Asymptotic preserving scheme for P_1 model

The idea is to derive from the previous scheme a scheme for the P_1 system. We want this scheme to tend to the Breil-Maire or MPFA-O scheme in the diffusion limit.

The first and the third relations are the same as in the diffusion scheme. The second relation is a centered discretization of the second equation of (6). The last relations are obtained by the conservation of the Riemann invariants of the P_1 system similar to the Eucclyd scheme [MABO07] for the Euler equations.

$$\begin{cases} \mid \Omega_j \mid \partial_t E_j(t) + \displaystyle\sum_r \frac{1}{2\varepsilon}(l_{jr-1,r}\Phi^j_{r-1/2,r} + l_{jr,r+1}\Phi^j_{r,r+1/2}) = 0 \\ \mid \Omega_j \mid \partial_t \mathbf{F}_j(t) + \displaystyle\sum_r \frac{1}{2\varepsilon}(l_{jr-1,r}\mathbf{n}_{jr-1,r}\bar{E}_{r-1/2,r} + l_{jr,r+1}\mathbf{n}_{jr,r+1}\bar{E}_{r,r+1/2}) = -\frac{\sigma}{\varepsilon^2} \mid \Omega_j \mid \mathbf{F}_j \\ \frac{1}{2}l_k(\Phi_k^{k-1} + \Phi_k^k) = 0 \\ \bar{E}_{r-1/2,r} - E_j + (\Phi^j_{r-1/2,r} - \mathbf{F}_j \cdot \mathbf{n}_{jr-1,r}) = 0 \\ \bar{E}_{r,r+1/2} - E_j + (\Phi^j_{r,r+1/2} - \mathbf{F}_j \cdot \mathbf{n}_{jr,r+1}) = 0 \end{cases} \tag{28}$$

This scheme has not the diffusion limit. To obtain this property, one uses the Jin-Levermore procedure. It consists in replacing E_j in the fourth relation (resp the last one) by $E_j+(\bar{E}_{r-1/2,r}-E_j)$ (resp $E_j+(\bar{E}_{r,r+1/2}-E_j)$) where $(\bar{E}_{r-1/2,r}-E_j)$ (resp $(\bar{E}_{r+1/2,r}-E_j)$) is given by the relations of the previous diffusion schemes. This manipulation is equivalent to incorporate the source term in the fluxes as for the GLACE AP scheme [BDF10] with the Jin-Levermore procedure.

$$\begin{pmatrix} \bar{E}_{r-1/2,r}-E_j \\ \bar{E}_{r,r+1/2}-E_j \end{pmatrix} = -\begin{pmatrix} \dfrac{2\omega_r^j}{l_{jr-1,r}} & 0 \\ 0 & \dfrac{2\omega_r^j}{l_{jr,r+1}} \end{pmatrix} (T_r^j)^{-1}\frac{\sigma}{\varepsilon}\begin{pmatrix} \Phi^j_{r-1/2,r} \\ \Phi^j_{r,r+1/2} \end{pmatrix} \tag{29}$$

Consequently the two last scalar relations of (28) are replaced by a linear system obtained by plugging (29) in these relations. One gets finally

Definition 8. *The P_1 AP scheme is*

$$\begin{cases} \mid \Omega_j \mid \partial_t E_j(t) + \displaystyle\sum_r \frac{1}{2\varepsilon}(l_{jr-1,r}\Phi^j_{r-1/2,r} + l_{jr,r+1}\Phi^j_{r,r+1/2}) = 0 \\ \mid \Omega_j \mid \partial_t \mathbf{F}_j(t) + \displaystyle\sum_r \frac{1}{2\varepsilon}(l_{jr-1,r}\mathbf{n}_{jr-1,r}\bar{E}_{r-1/2,r} + l_{jr,r+1}\mathbf{n}_{jr,r+1}\bar{E}_{r,r+1/2}) = -\frac{\sigma}{\varepsilon^2} \mid \Omega_j \mid \mathbf{F}_j, \\ \dfrac{1}{2} l_k(\Phi_k^{k-1} + \Phi_k^k) = 0 \\ \begin{pmatrix} \Phi^j_{r-1/2,r} \\ \Phi^j_{r,r+1/2} \end{pmatrix} = -\dfrac{1}{2\omega_r^j}\tilde{M}_r^j \begin{pmatrix} l_{jr-1,r}(\bar{E}_{r-1/2,r}-E_j) - l_{jr-1,r}(\mathbf{F}_j,\mathbf{n}_{jr-1,r}) \\ l_{jr,r+1}(\bar{E}_{r,r+1/2}-E_j) - l_{jr,r+1}(\mathbf{F}_j,\mathbf{n}_{jr,r+1}) \end{pmatrix} \end{cases} \tag{30}$$

with

$$\tilde{M}_r^j = 2\omega_r^j \begin{pmatrix} l_{jr-1,r}(1+(S^j_{r,\epsilon})^{xx}) & l_{jr-1,r}(S^j_{r,\epsilon})^{xy} \\ l_{jr,r+1}(S^j_{r,\epsilon})^{yx} & l_{jr,r+1}(1+(S^j_{r,\epsilon})^{yy}) \end{pmatrix}^{-1} \tag{31}$$

$$S^j_{r,\epsilon} = \begin{pmatrix} \dfrac{2\omega_r^j}{l_{jr-1,r}} & 0 \\ 0 & \dfrac{2\omega_r^j}{l_{jr,r+1}} \end{pmatrix} \frac{\sigma}{\epsilon}(T_r^j)^{-1} \tag{32}$$

and T_r^j the local matrix associated to the Breil-Maire or MPFA-O scheme.

As in the previous scheme, the auxiliary unknowns can be eliminated leading to a centered scheme with 3 unknowns per cell E_j, F_j^x, F_j^y. In the case of a structured mesh composed of quadrilaterals, the scheme has a nine points stencil, each point becoming now a block of three variables.

Proposition 9. *The asymptotic limit of the scheme (30-31-32) is the Breil-Maire scheme if we choose for T_r^j the local matrix (22), and the MPFA-O scheme if we choose for T_r^j the local matrix (24).*

Proof. As for the AP GLACE scheme we use a Hilbert expansion to prove the result.

$$E_j = E_j^0 + \varepsilon E_j^1 + \varepsilon^2 E_j^2 ....$$

$$E_{r\pm\frac{1}{2},r} = E^0_{r\pm\frac{1}{2},r} + \varepsilon E^1_{r\pm\frac{1}{2},r} + \varepsilon^2 E^2_{r\pm\frac{1}{2},r} ....$$

We do the same for all other variables and fluxes. Plugging the previous expansion in the scheme we obtain for the first equation
The term proportional to $\frac{1}{\varepsilon}$

$$\sum_r \frac{1}{2}(l_{jr-1,r}\Phi^{j,0}_{r-1/2,r} + l_{jr,r+1}\Phi^{j,0}_{r,r+1/2}) = 0 \tag{33}$$

The term proportional to $\frac{1}{\varepsilon^0}$

$$\partial_t E_j^0(t) + \sum_r \frac{1}{2}(l_{jr-1,r}\Phi^{j,1}_{r-1/2,r} + l_{jr,r+1}\Phi^{j,1}_{r,r+1/2}) = 0. \tag{34}$$

We use the same process for the second equation

$$\frac{1}{\varepsilon^2}: \qquad \mathbf{F}_j^0 = 0, \tag{35}$$

$$\frac{1}{\varepsilon^1}: \qquad \sum_r \frac{1}{2}(l_{jr-1,r}\mathbf{n}_{jr-1,r}\bar{E}^0_{r-1/2,r} + l_{jr,r+1}\mathbf{n}_{jr,r+1}\bar{E}^0_{r,r+1/2}) = -\sigma \mid \Omega_j \mid \mathbf{F}_j^1, \tag{36}$$

$$\frac{1}{\varepsilon^0}: \qquad \mid \Omega_j \mid \partial_t \mathbf{F}_j^0(t) + \sum_r \frac{1}{2}(l_{jr-1,r}\mathbf{n}_{jr-1,r}\bar{E}^1_{r-1/2,r} + l_{jr,r+1}\mathbf{n}_{jr,r+1}\bar{E}^1_{r,r+1/2}) = -\sigma \mid \Omega_j \mid \mathbf{F}_j^2. \tag{37}$$

After using the Hilbert expansion, we rewrite the equation on the fluxes Φ.

$$\begin{pmatrix} l_{jr-1,r}(1+(S^j_{r,\epsilon})^{xx}) & l_{jr-1,r}(S^j_{r,\epsilon})^{xy} \\ l_{jr,r+1}(S^j_{r,\epsilon})^{yx} & l_{jr,r+1}(1+(S^j_{r,\epsilon})^{yy}) \end{pmatrix} \begin{pmatrix} \Phi^j_{r-1/2,r} \\ \Phi^j_{r,r+1/2} \end{pmatrix} \tag{38}$$

$$= -\begin{pmatrix} l_{jr-1,r}(\bar{E}_{r-1/2,r} - E_j) - l_{jr-1,r}(\mathbf{F}_j, \mathbf{n}_{jr-1,r}) \\ l_{jr,r+1}(\bar{E}_{r,r+1/2} - E_j) - l_{jr,r+1}(\mathbf{F}_j, \mathbf{n}_{jr,r+1}) \end{pmatrix} \tag{39}$$

As before, we plug the Hilbert expansion in the formula.

$$\frac{1}{\varepsilon^1}: \qquad 2w_r^j\sigma(T_r^j)^{-1}\begin{pmatrix} \Phi^{j,0}_{r-1/2,r} \\ \Phi^{j,0}_{r,r+1/2} \end{pmatrix} = 0, \tag{40}$$

$$\frac{1}{\varepsilon^0}: \qquad \begin{pmatrix} l_{jr-1,r} & 0 \\ 0 & l_{jr,r+1} \end{pmatrix}\begin{pmatrix} \Phi^{j,0}_{r-1/2,r} \\ \Phi^{j,0}_{r,r+1/2} \end{pmatrix} + 2w_r^j\sigma(T_r^j)^{-1}\begin{pmatrix} \Phi^{j,1}_{r-1/2,r} \\ \Phi^{j,1}_{r,r+1/2} \end{pmatrix}$$

$$= -\begin{pmatrix} l_{jr-1,r}(\bar{E}^0_{r-1/2,r} - E_j^0) - l_{jr-1,r}(\mathbf{F}_j^0, \mathbf{n}_{jr-1,r}) \\ l_{jr,r+1}(\bar{E}^0_{r,r+1/2} - E_j^0) - l_{jr,r+1}(\mathbf{F}_j^0, \mathbf{n}_{jr,r+1}). \end{pmatrix} \tag{41}$$

The equation (40) gives

$$\begin{pmatrix} \Phi^{j,0}_{r-1/2,r} \\ \Phi^{j,0}_{r,r+1/2} \end{pmatrix} = 0. \tag{42}$$

Therefore, using (42), (35), (34) and (41) we obtain

$$\begin{cases} \mid \Omega_j \mid \partial_t E_j^0(t) + \sum_r \frac{1}{2}(l_{jr-1,r}\Phi^{j,1}_{r-1/2,r} + l_{jr,r+1}\Phi^{j,1}_{r,r+1/2}) = 0 \\ \begin{pmatrix} \Phi^{j,1}_{r-1/2,r} \\ \Phi^{j,1}_{r,r+1/2} \end{pmatrix} = -\frac{1}{\sigma}\frac{1}{2\omega_r^j}T_r^j \begin{pmatrix} l_{jr-1,r}(\bar{E}^0_{r-1/2,r} - E_j^0) \\ l_{jr,r+1}(\bar{E}^0_{r,r+1/2} - E_j^0) \end{pmatrix} \end{cases}$$

To finish we develop the continuity condition, using (42) in the third equation of (30) and simplify by ε, we obtain

$$\frac{1}{2}l_k(\Phi_k^{k-1,1} + \Phi_k^{k,1}) = 0$$

This result ends the proof. □

4. Numericals results

4.1. Test 1

We propose a test detailed in [BM06]. This test involves an analytical solution of a diffusion equation. Thus, it allows to determine numerically the order of accuracy of the diffusion schemes on various meshes. This test will also assert the asymptotic preserving property of the schemes studied for the P_1 model.

We solve the following stationary diffusion equation

$$-\Delta E_{stat} = Q$$

with $x \in [0,1]$ and $y \in [0,1]$, and as boundary conditions
$\frac{\partial E_{stat}}{\partial x}(x=0,y)=0$, $\frac{\partial E_{stat}}{\partial x}(x=1,y)=0$, $\frac{\partial E_{stat}}{\partial y}(x,y=0)=0$ and $\frac{\partial E_{stat}}{\partial y}(x,y=1)=0$.

The source term is $Q(x,y) = (\frac{cos(1)-1}{sin(1)})cos(x) + sin(x)$.

The solution depends only on x and is defined at an additive constant. We look for
$E_{stat}(x,y) = -x + (\frac{cos(1)-1}{sin(1)})cos(x) + sin(x) + 0.5$ whose integral is null.

To obtain the solution of this stationary diffusion equation, we look for the solution of the following unsteady diffusion equation

$$\frac{\partial E}{\partial t} - \Delta E = Q$$

with $E(x,y,t=0)=0$, $\frac{\partial E}{\partial x}(x=0,y,t)=0$, $\frac{\partial E}{\partial x}(x=1,y,t)=0$, $\frac{\partial E}{\partial y}(x,y=0,t)=0$ and $\frac{\partial E}{\partial y}(x,y=1,t)=0$. It tends to E_{stat} when t tends to infinity since the integral of Q is null.

First, the errors in L^2 norm in function of the diameter h of the mesh are compared for the GLACE, Breil-Maire and MPFA-O diffusion schemes on two types of meshes, the Kershaw mesh and a random mesh.

On the Kershaw mesh (Fig. 5 left), as expected, all the diffusion schemes exhibit a second order convergence with a smaller constant of convergence for MPFA-O. On the random mesh (Fig. 5 right), the Breil-Maire scheme does not converge as it has already been observed [BM06] and the MPFA-O scheme converges with a second order like the GLACE scheme.

We have also compared the Breil-Maire diffusion scheme and the MPFA-O diffusion scheme on the triangular mesh obtained from a quadrilateral mesh by joining in each quadrilateral the isobarycenter to its four vertices. When this procedure is applied to the random meshes (Fig .6 left), we observe a second order convergence for the two schemes with very similar errors (Fig .6 right). It is surprising that the Breil-Maire scheme converges although it does not converge at all on the corresponding quadrilateral mesh. This point should be addressed in a future work. On the same case, the GLACE diffusion scheme does not converge. Spurious modes occur and we were not able to obtain a stationary solution. In other cases [BDF10], it has been reported that this scheme can converge on triangular meshes. The analysis of this behaviour is under study and a way to avoid these spurious modes will be proposed in the next future.

We compare the GLACE diffusion scheme and the MPFA-O scheme on a general polygonal mesh (cells having more than 4 edges are present) obtained from an hydrodynamic calculation (Fig .7). We obtain a good agreement (Fig .8) between the two schemes. The error values of the MPFA-O and the GLACE diffusion schemes are respectively 3.07952×10^{-5} and 3.63853×10^{-5}. The Breil-Maire scheme error value is much larger: 6.3×10^{-4}.

We have compared the Breil-Maire diffusion scheme and the MPFA-O scheme on the triangular mesh (Fig .9). The error values of the MPFA-O schemes and the Breil-Maire scheme are respectivly 2.7217×10^{-6} and 6.15042×10^{-6}. We plot the MPFA-O solution on (Fig .10).

We are also interested in E_ε solution of the P_1 system :

$$\begin{cases} \partial_t E_\varepsilon + \dfrac{1}{\varepsilon}\nabla.\mathbf{F}_\varepsilon = Q \\ \partial_t \mathbf{F}_\varepsilon + \dfrac{1}{\varepsilon}\nabla.(E_\varepsilon I_d) = -\dfrac{1}{\varepsilon^2}\mathbf{F}_\varepsilon \end{cases}$$

with the boundary conditions $F_\varepsilon(x=0,y,t)=0$, $F_\varepsilon(x=1,y,t)=0$, $F_\varepsilon(x,y=0,t)=0$ and $F_\varepsilon(x,y=1,t)=0$.

When ε tends to zero, E_ε tends towards the solution of the unsteady diffusion equation $\dfrac{\partial E}{\partial t} - \Delta E = Q$. Then, if as predicted, the three schemes for the P_1 model are AP, they must give the same solutions as their asymptotic diffusion limit schemes when ε tends to zero.

On the same figures, we have plotted the errors between the stationary solutions obtained with the P_1 GLACE, P_1 Breil-Maire and P_1 MPFA-O schemes for $\varepsilon = 0.001$ and E_{stat}. As expected, as long as the diffusion limit is valid, said as long as $\frac{h}{\varepsilon}$, which represents the number of mean free paths per cell, is large enough, the three schemes give almost same solutions as their asymptotic limit. We thus obtain a second order convergence for the three schemes on the Kershaw mesh, a second order convergence for the P_1 GLACE and P_1 MPFA-O on the random mesh. We observe on this mesh a non monotone behaviour of the error with the P_1 Breil-Maire scheme. On the first crude random meshes, the error is almost constant. It begins to decrease very slowly when the mesh is so refined that the diffusion limit becomes no longer valid.

We are also interested in the behaviour of the schemes for ε not small. E_ε tends to E_{stat} when t tends to infinity whatever ε is. Thus we can compare the stationary solution of the schemes with E_{stat}. We set $\varepsilon = 1$. In this case (Fig. 11), the diffusion limit is not valid and an order of convergence close to one is obtained for the three schemes on the Kershaw mesh and the random mesh. On these cases, the P_1 Breil-Maire and the P_1 MPFA-O schemes give indistinguishable results. Note that the P_1 Breil-Maire scheme converges at order one on the random mesh because this is not the diffusion but the "acoustic" part of the scheme which is now involved. For all the P_1 schemes, some kind of slope reconstruction would be necessary to get a second order but it has not yet been done.

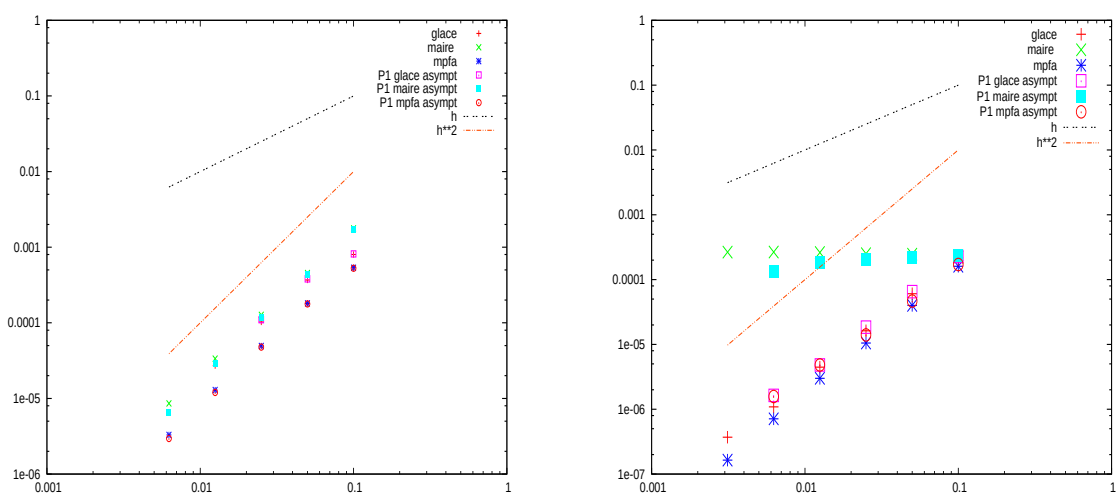

FIGURE 5. Diffusion case : convergence on the Kershaw mesh on the left and on a random mesh on the right

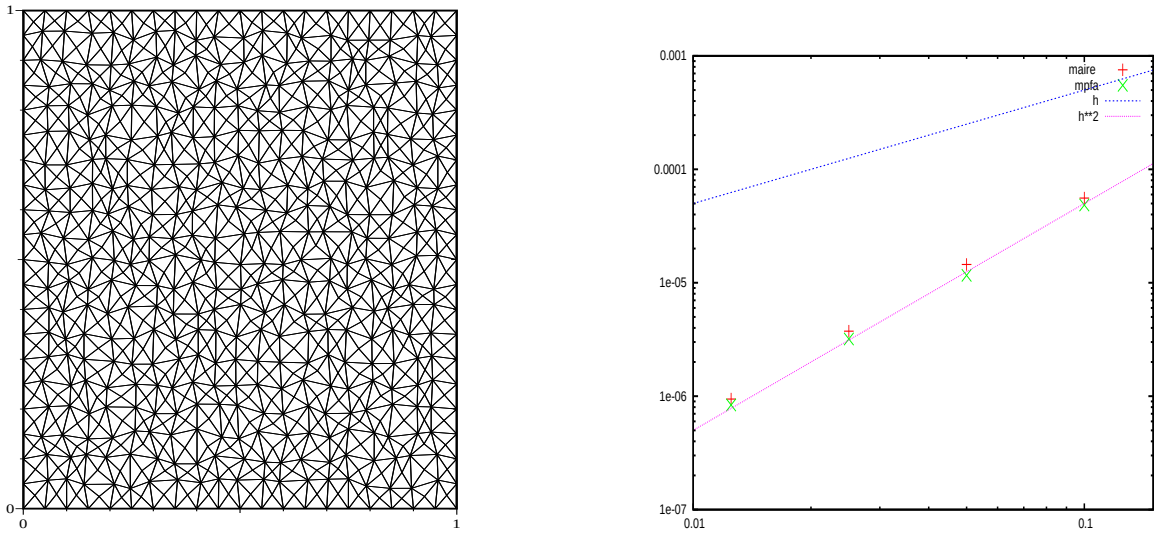

FIGURE 6. Diffusion case : triangular mesh on the left and convergence on the triangular mesh on the right

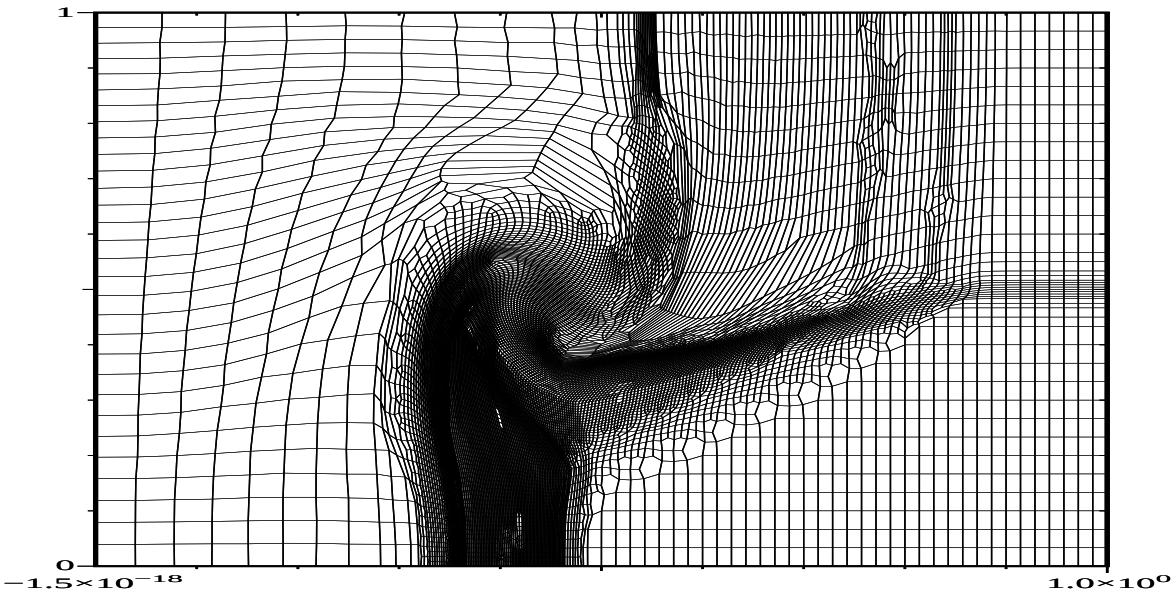

FIGURE 7. polygonal unstructured mesh.

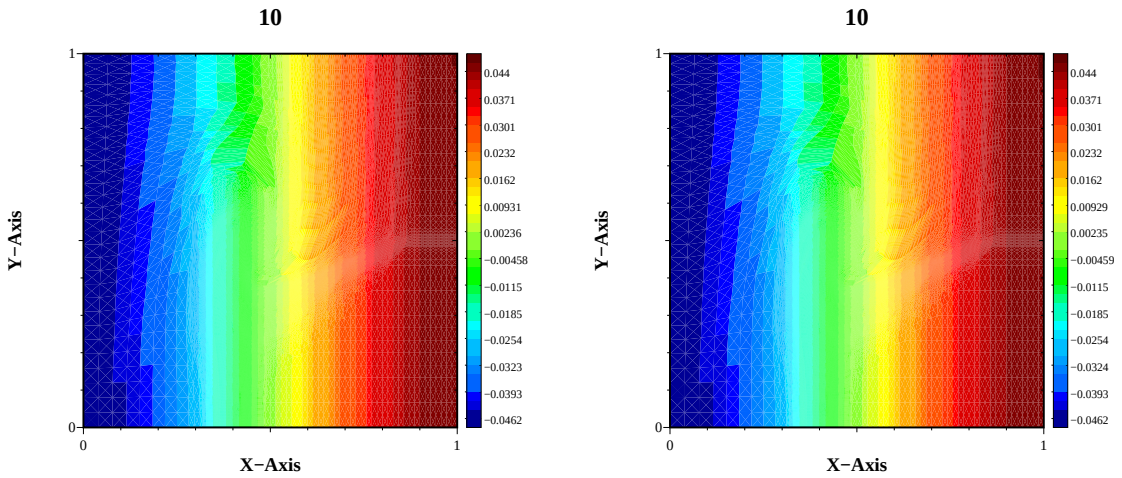

FIGURE 8. Solution of the diffusion test on the mesh (Fig. 7) for GLACE in the left, for MPFA-O in the right.

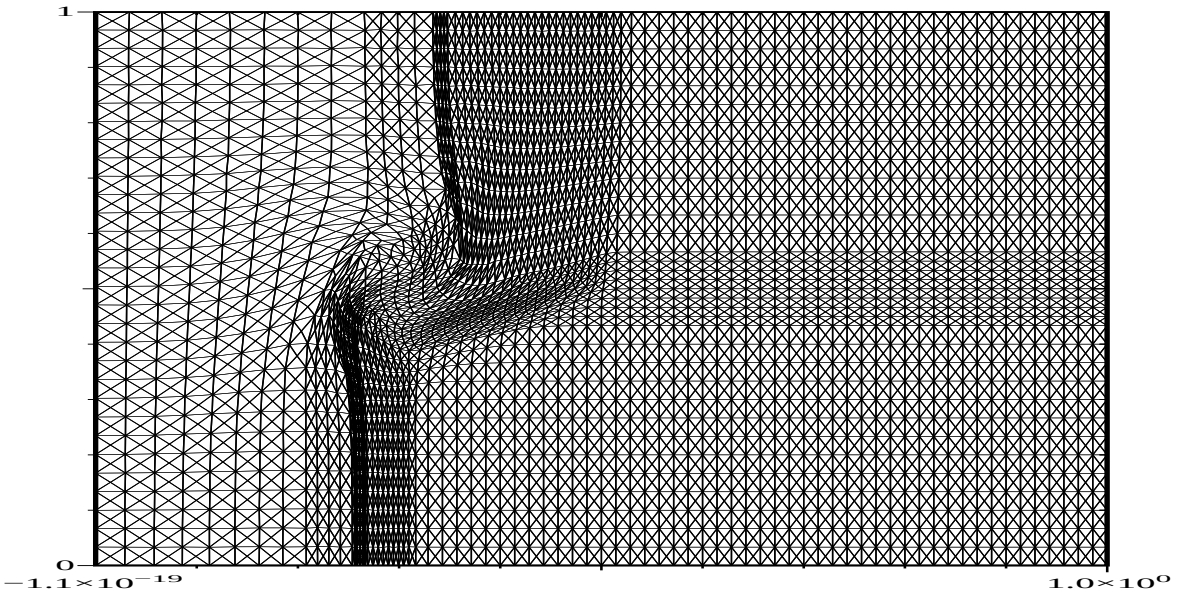

FIGURE 9. triangular mesh.

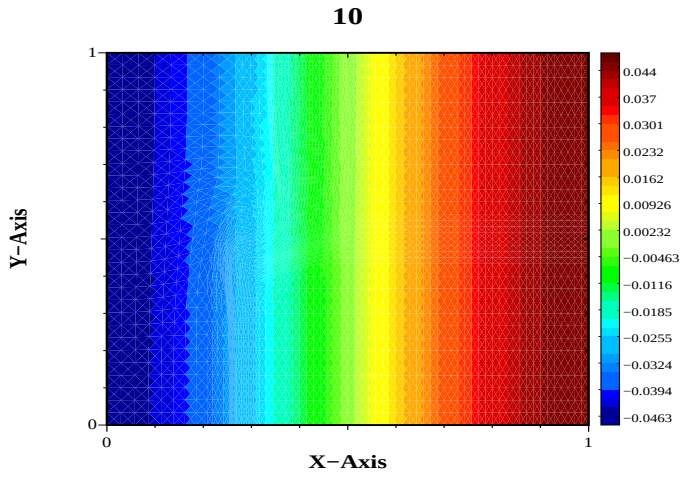

FIGURE 10. Solution of the diffusion test on the triangular mesh (Fig. 9) for MPFA-O.

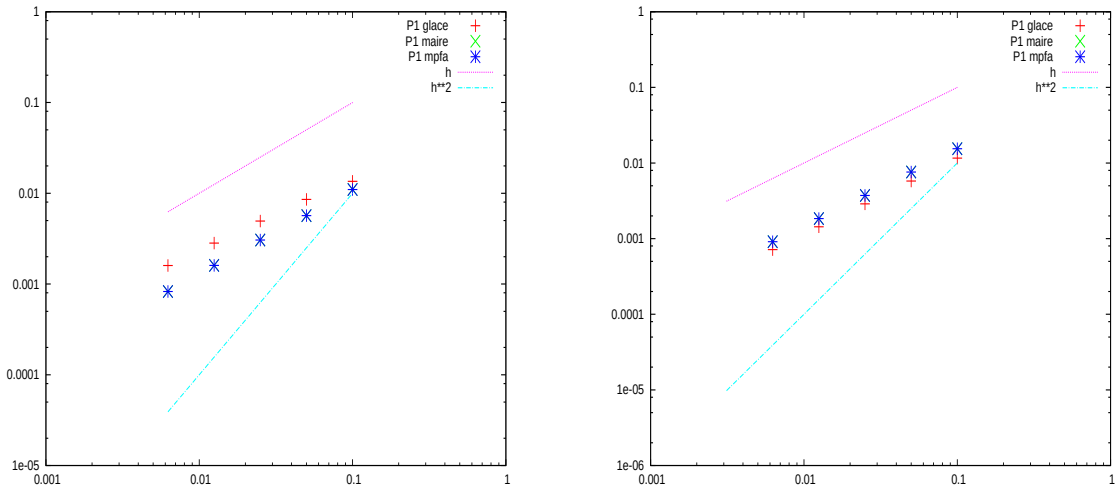

FIGURE 11. Transport case Convergence on the Kershaw mesh on the left and on a random mesh on the right

4.2. **Test 2**

The purpose of this difficult test is to valid the P_1 model discretization in the transport regime.

The line source problem we are interested in consists in imposing a Dirac function at $t = 0$ located at (x_c, y_c) and looking for the P_1 unsteady solution with $\sigma_t = 1$ and $\varepsilon = 1$. The $E(r,t)$ exact solution [MC08] where $r = \sqrt{(x-x_c)^2 + (y-y_c)^2}$ is the distance to the source is composed of a Dirac function in r which propagates at the speed $v = 1$ plus a smooth function between $r = 0$ and $r = t$. At $t = 1$ the smooth part is negative and becomes positive at later times. This failure is due to the fact that at earlier times, the initial source particles have not suffered much collisions and the solution is strongly anisotropic. Therefore, the transport solution cannot be represented accurately by the P_1 model. We have meshed a square $[0,4] \times [0,4]$ with a very fine cartesian mesh $nx = ny = 800$ and taken a small time step $\Delta t = 0.0025$. The boundary conditions are symmetry conditions ($\mathbf{F}.\mathbf{n} = 0$). The Dirac function at the center $x_c = y_c = 2$ at $t = 0$ is approximated by the characteristic function of the center cell divided by $\Delta x \Delta y$.
On the figure 12, we have plotted at $t = 1$ the P_1 MPFA-O solution and the exact solution computed by Delyan Zhelyazov with Mathematica (the Dirac function here is represented by a straight line of equation $r = 1$). If the solution was perfectly symmetric, the solution would depend only on r. It is not true in our case since the mesh does not respect this symmetry (a polar mesh should be used instead of a cartesian mesh). Therefore, we have plotted all the values of the calculated solution in function of r which explains why the calculated solution is multivalued. The agreement with the exact solution is very satisfactory despite the singularity of the initial condition and the order one accuracy of this scheme. Similar results were obtained on the same problem in [BH05] with Riemann type schemes. The 1D cylindrical symmetry is well preserved and is lost only close to the center.

We have also computed the solution on a random mesh cruder than the previous one ($nx = ny = 100$) with $\Delta t = 0.01$.

This is a very difficult test for the P_1 GLACE scheme because of its cross stencil on cartesian meshes. Despite the mesh is not cartesian, spurious modes are still present in the solution (Fig. 13) which is not the case for the P_1 MPFA-O solution.

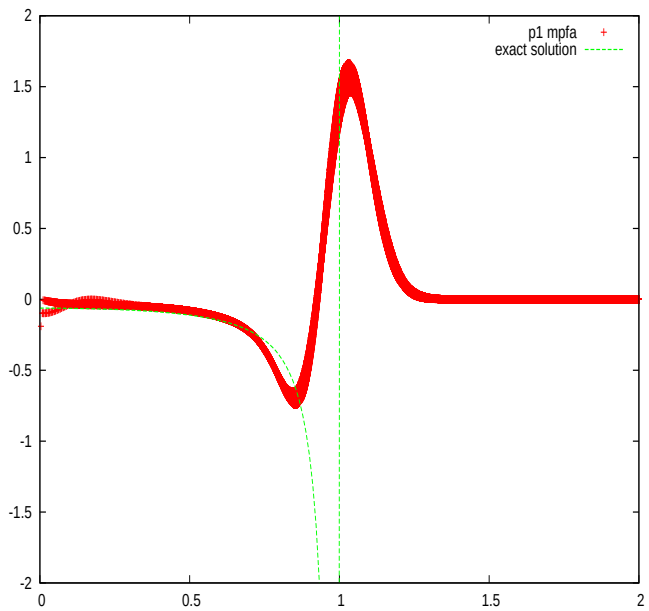

FIGURE 12. comparison of the P_1 MPFA-O solution with the exact solution at t=1

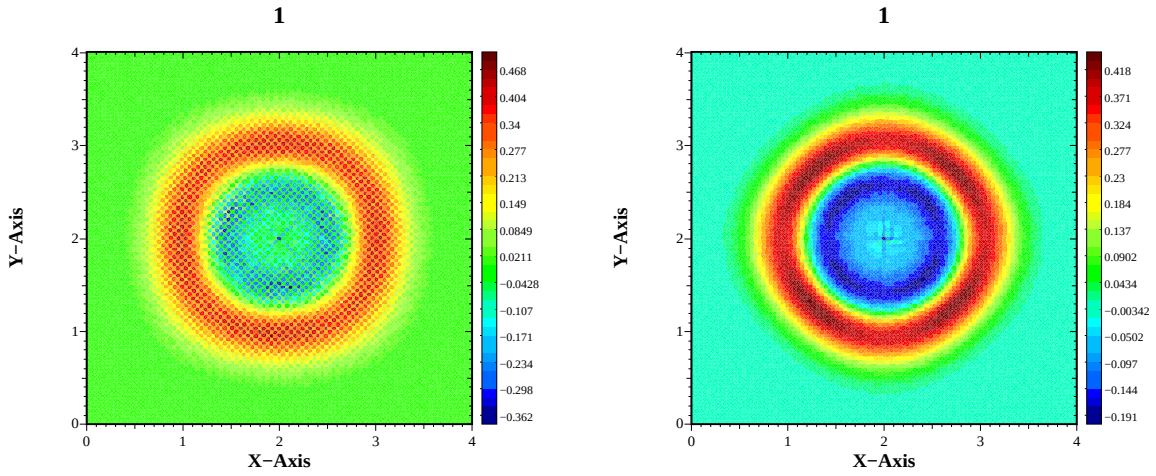

FIGURE 13. left solution P_1 GLACE solution, right P_1 MPFA-O solution

5. Conclusion

The goals of this project reported in this paper were multiple :

- Study the behaviour of some existing schemes for the diffusion equation on general unstructured polygonal meshes.

  We have compared the Breil-Maire scheme, one more accurate variant and a new diffusion scheme inspired by the GLACE scheme for Euler equations. We discovered that the variant of the Breil-Maire scheme was the MPFA-O scheme. Orders of convergence are reported on various meshes. Calculations on polygonal meshes issued from hydrodynamic calculation prove their ability to solve the diffusion equation on general Arbitrary Lagrangian polygonal Meshes.
- Test a recent scheme for solving the P_1 system on this type of meshes.

  Before this study, a scheme for solving the P_1 system on unstructured meshes was designed. This scheme was also inspired by the GLACE scheme for Euler equations. Its diffusion limit is the previous mentioned diffusion scheme. We verified numerically this property is true on polygonal meshes. It was known that it can exhibit spurious modes on cartesian meshes and we found the same pathology on some triangular meshes.
- Propose new schemes for solving the P_1 system which do not have this default.

  For this purpose, we have designed two new schemes ; the first one has the Breil-Maire scheme for diffusion limit and the second one has the MPFA-O scheme for diffusion limit. On a first test, we have demonstrated numerically they are AP. A second test has been proposed to assert their behaviour in the transparent regime. Each of these schemes have pro and cons. The choice will depend on the involved case.

But the P_1 model does not allow a large anisotropy of the radiative intensity, more accurate closures such as the M_1 model are needed to give accurate solutions of ICF experiments. Studies will continue in this way.

6. Acknowledgments

We would like to thank Delyan Zhelyazov for computing the analytical Green's function which helped us to valid our method and Georges Sadaka who brought us in time a FreeFem++ solution for this problem.

References

[ABBM98] I. Aavatsmark, T. Barke, O. Boe, T. Mannseth, *Discretization on unstructured grids for inhomogeneous anisotropic media. Part I: derivation of the methods.* SIAM J. Sci. Comput, Vol 19, No. 5, pp. 1700-1716, September 1998.

[AE06] I. Aavatsmark, G. T. Eigestad, *Numerical convergence of the MPFA O-method and U-method for general quadrilateral grids.* Int. J. Numer. Meth Fluids 2006; 51:939-961.

[Hoc02] J.D. Benamou P. Hoch, *GO++ : A modular lagrangian/eulerian software for hamilton jacobi equations of geometric optics type,* M2AN, 36(5):883-905, 2002.

[BCT08] C. Berthon, P. Charrier, R. Turpault, *An HLLC scheme to solve the M_1 model of radiative transfer in two dimensions* J. Sci. Comput., 31, no. 3, pp. 347-389, 2007.

[BOP07] F. Bouchut, H. Ounaissa, B. Perthame, *Upwinding of the source term at interfaces for Euler equations with high friction.* Computers and Mathematics with Applications, 53(3-4):361–375, 2007.

[BM06] J. Breil, P-H. Maire, *A cell-centered diffusion scheme on two-dimensional unstructured meshes.* Journal of Computational Physics 224 (2007) 785-823.

[BH05] T.A. Brunner, J.P. Holloway, *Two-dimensional time dependent Riemann solvers for neutron transport* Journal of Computational Physics 210 (2005) 386-399.

[BC07] C. Buet, S. Cordier, *An asymptotic preserving scheme for hydrodynamics radiative transfer models: numerics for radiative transfer.* Numer. Math., 108, 199-221 (2007).

[BD06] C. Buet, B. Després, *Asymptotic preserving and positive schemes for radiation hydrodynamics.* Journal of Computational Physics 2006, vol. 215, no2, pp. 717-740.

[BDF10] C. Buet, B. Després, E. Franck, *Design of asymptotic preserving scheme for the hyperbolic heat equation on unstructured Meshes.* preprint, report LJLL, UMPC, 2010.

[CDDL09] G. Carré, S. Del Pino, B. Després, E. Labourasse, *A Cell-centered lagrangian hydrodynamics scheme on general unstructured meshes in arbitrary dimension.* Journal of Computational Physics 228 (2009) no14, pp. 5160-518.

[CM08] J. Cartier, A. Munier, *Geometric Eddington factor for radiative transfer problems* in: CEMRACS 2003 Proceedings, IRMA Series in Mathematics and Theoretical Physics (EMS).

[CGRS08] F. Coquel, E. Godlewski, P.-A. Raviart, N. Seguin, *An asymptotic preserving scheme for Euler equations with gravity and friction* Finite volumes for complex applications V, Aussois, France, 8-13 juin 2008, pages 305-312, ISTE, Londres.

[DL04] J.D. Densmore, E.W. Larsen, *Asymptotic equilibrium diffusion analysis of time-dependent Monte Carlo methods for grey radiative transfer* Journal of Computational Physics 199 (2004) 175-204.

[DF99] B. Dubroca, J.L. Feugeas, *Hiérarchie des modèles aux moments pour le transfert radiatif.* C. R. Acad. Sci. Paris t.329, serie I,p.915-920,1999.

[FC71] J.A. Fleck, J.D. Cummings, *An implicit Monte-Carlo scheme for calculating time and frequency dependent radiation transport*, Journal of Computational Physics 8 (1971) 313.

[GT02] L. Gosse, G. Toscani, *An asymptotic-preserving well-balanced scheme for the hyperbolic heat equations.* C. R. Acad. Sci Paris,Ser. I 334 (2002) 337-342.

[Gos10] L. Gosse, *Asymptotic preserving and well-balanced scheme for the 1D Cattaneo model of chemotaxis movement in both hyperbolic and diffusive regimes* Preprint HAL : hal-00528684.

[Hoc11] P. Hoch, *Discontinuous ALE in order to modelize adaptation of polygonal meshes without exact intersection calculation,* in preparation.

[JL96] S. Jin, D. Levermore, *Numerical schemes for hyperbolic conservation laws with stiff relaxation terms.* Journal of Computational Physics 126,449-467 , 1996.

[MABO07] P-H. Maire, R. Abgrall, J. Breil, J. Ovadia, *A cell-centered lagrangian scheme for two-dimensional compressible flow problems.* SIAM J. Sci. Comput. Vol 29,No. 4, pp. 1781-1824. 2007.

[Maz07] C. Mazeran, *Sur la structure mathématique et l'approximation numérique de l'hydrodynamique lagrangienne bidimensionnelle.* PhD thesis, University of Bordeaux, 2007.

[MC08] R.G. McClarren, J.P. Holloway, T.A. Brunner, *Analytical P_1 solutions for time-dependent, thermal radiative transfer in several geometries.* Journal of Quantitative Spectroscopy and Radiative Transfer 109 389-403 (2008) 389-403.

[MV06] M. Vohralik, *Equivalence between lowest-order mixed finite element and multi-point finite volume methods on simplicial meshes.* ESAIM: M2AN Vol. 40, No 2, 2006, pp. 367-391.